J. Fluid Mech. (1981), *vol.* 109, *pp.* 125–146
Printed in Great Britain

The influence of mean shear on unsteady aperture flow, with application to acoustical diffraction and self-sustained cavity oscillations

By M. S. HOWE
Bolt Beranek and Newman, Inc., 50 Moulton Street, Cambridge, MA 02138, U.S.A.

(Received 4 February 1980)

This paper discusses the linearized theory of unsteady flow through a two-dimensional aperture in a thin plate in the presence of a grazing mean flow on one side of the plate. The mean shear layer is modelled by a vortex sheet, and it is predicted that at low mean-flow Mach numbers there is a transfer of energy from the mean flow to the disturbed motion of the vortex sheet provided (i) the Kutta condition is imposed at the leading edge of the aperture, resulting in the unsteady shedding of vorticity from the edge, and (ii) the width of the aperture $2s$ satisfies $\frac{1}{2} < 2s/\lambda < 1{\cdot}1$, where λ is the hydrodynamic wavelength of the disturbance on the vortex sheet within the aperture. The theory is used to examine the effect of mean shear on the diffraction of sound by a perforated screen, and to predict the spontaneous excitation and suppression of self-sustained oscillations in a wall-cavity beneath a nominally steady mean flow. In the latter case support for the proposed theory is provided by a favourable comparison of theoretical results with experimental data available in the literature.

1. Introduction

Sound incident on a rigid body generates vorticity and results in a transfer of energy from a compressible mode of fluid motion to one associated with the essentially incompressible induced velocity field of the vorticity distribution. This mechanism of acoustic attenuation is exploited in engineering practice by the deployment of perforated screens or acoustic liners, wherein unsteady 'jetting' of fluid in surface apertures leads to an enhanced conversion of energy from the acoustic to the vortical mode. Moreover, the experiments of Barthel (1958), Bechert, Michel & Pfizenmaier (1977) and Bechert (1979) demonstrate that the presence of a *mean* flow through a perforated screen or liner further increases the possible levels of attenuation, as vorticity generated at the edges of the apertures is convected away in the flow into regions where it is unable to interact effectively with the sound, and where its energy is dissipated as heat. Several idealized model problems have been examined (Howe 1979*a*, *b*, 1980*a*, *b*) in order to estimate theoretically the influence of the mean flow in such cases. In particular Howe (1980*a*) has discussed the attenuation which occurs when sound impinges on a screen which is perforated by a series of parallel, equal and equidistant slits in the presence of a uniform *tangential* mean flow which is the same on both sides of the screen. The coupling between the acoustic and vortical fields is effected analytically by the application of the Kutta condition at the sharp leading edges of the slits (A in figure 1), in the manner of unsteady thin airfoil theory (Ashley &

Landahl 1965, § 13.2), and in appropriate circumstances it is predicted that up to 50 % of the incident acoustic energy can be lost during the interaction with the screen.

The situation may be expected to differ significantly when the magnitude of the tangential mean flow velocity is different on opposite sides of the screen. In the limiting case of an ideal fluid, a vortex sheet in the plane of the slits will separate the two mean flows. The sheet is unstable, and an incident sound wave will initiate the growth of the characteristic Kelvin–Helmholtz instability waves at the leading edges of the slits. The subsequent interaction of these waves with the downstream edges will involve the generation of acoustic disturbances (aerodynamic sound). Since the amplitude of an instability wave increases as it propagates across the slit, it is possible that under certain conditions the screen will behave as a net source of acoustic energy.

The general question of the role of shear-layer instabilities in acoustic problems has received extensive attention in the literature in connection with edge tones (see e.g. Rockwell & Naudascher 1979), and self-sustained resonant oscillations caused by grazing flow over a cavity in a wall (Rossiter 1962; Covert 1970; DeMetz & Farabee 1977; Elder 1978; Tam & Block 1978). Analogous problems arise in the excitation of standing acoustic waves in organ pipes and musical instruments such as the flute (cf. Fletcher 1979), and in the classical edge tone (Crighton & Innes 1981).

The theoretical problem of calculating the interaction of sound with a shear layer in the presence of rigid boundaries is difficult, and at some stage most theoretical models resort to the empirical fitting of adjustable constants. Heller & Bliss (1975) and Tam & Block (1978), for example, invoke the existence of an acoustic source in the vicinity of the downstream edge, where the disturbed motion of the shear layer is particularly intense. Similarly, Elder (1978), Tam & Block (1978) and Fletcher (1979) ignore the influence of the downstream edge in calculating the disturbed motion of the shear layer, and erroneously assume that the lateral displacement of the layer is equal to a linear combination of Kelvin–Helmholtz modes (modified, perhaps, to allow for a finite width of the layer) together with a component arising from the net acoustic flux through the slit or aperture.

The validity of the various approximate analyses could possibly be assessed if exact solutions were available in certain limiting situations. Möhring (1975) has proposed an elegant function-theoretic treatment of linearly perturbed vortex sheets in incompressible flow in the presence of edges and slit apertures. The predictions of this analysis do not appear to be relevant to real, unsteady aperture flows, however, since the displacement of the vortex sheet is required to vary continuously at the leading and trailing edges of the aperture, and this apparently prevents an application of the Kutta condition at the upstream edge. On the linear theory of an ideal fluid, a solution in which the Kutta condition is not satisfied does not include a mechanism by means of which energy can be transferred between an acoustic and a vortical field. The difficulty in Möhring's approach and, incidentally, in Covert's (1970) analysis of compressible cavity oscillations, arises from the condition that the displacement of the vortex sheet is required to tend continuously to zero at the trailing (i.e. downstream) edge. This is, of course, in conflict with *all* experimental observations, which reveal that conditions at the trailing edge are decidedly discontinuous and nonlinear. Nevertheless, it may be argued that a linear theory could still yield a valuable first approximation to the real situation provided that it incorporates some type of singular behaviour at the trailing edge. It is the purpose of this paper to propose such a theory.

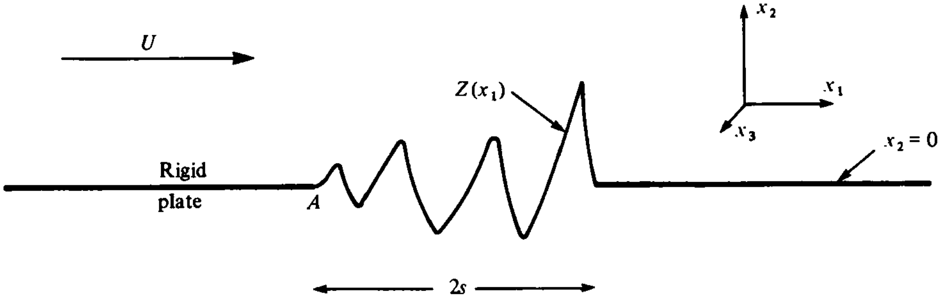

FIGURE 1. Schematic illustration of the canonical problem.

The theory is formulated in § 2 in terms of a two-dimensional canonical problem of unsteady flow through a slit aperture in a thin rigid plate. In the undisturbed state the slit is spanned by a vortex sheet which separates fluid in uniform motion on one side of the plate from fluid at rest on the other. Viscosity is neglected, except in so far as it is ultimately responsible for the production of vorticity in accordance with an application of the Kutta condition at the leading edge of the slit. It is shown that the displacement of the vortex sheet must exhibit an inverse square root singularity as the trailing edge is approached in order that a transfer of energy can occur between an imposed oscillatory motion (caused, for example, by an incident sound wave) and the mean flow. A range $\frac{1}{2}\pi < \epsilon < 3{\cdot}49$ of the reduced frequency $\epsilon = \omega s/U$ (ω being the angular frequency, s the half-width of the slit, and U the velocity of the uniform mean flow) is found within which the disturbed motion can extract energy from the mean flow. The transfer is greatest when $\epsilon = 2{\cdot}25$ when approximately $\frac{3}{4}$ of a wavelength of a vortex-sheet instability mode occupies the slit. This remarkable result was first observed experimentally by Rossiter (1962).

The theoretical results are applied in § 3 to the problem mentioned above of the diffraction of sound by a screen perforated by a series of parallel, equal and equidistant slits in the presence of a uniform mean flow on one side of the screen alone. The theory predicts significant departures from the case treated by Howe (1980*a*) in which the mean flow is the same on both sides of the screen. In § 4 the analysis is extended to model the problem of self-sustained wall-cavity oscillations. Encouraging support for the basis of the present treatment is provided in this case by a favourable comparison with published experimental data.

2. Analysis of unsteady aperture flow

In this section a generalized discussion is given of the effect of mean shear on the pulsatile flow of an ideal fluid through a sharp-edged slit. Consider the two-dimensional problem illustrated in figure 1. A thin rigid plate lies in the plane $x_2 = 0$ of a rectangular co-ordinate system (x_1, x_2, x_3), with the x_3 axis directed out of the plane of the paper in the figure. There is slit of width $2s$ which occupies the portion $(|x_1| < s, -\infty < x_3 < \infty)$ of the plate. In the undisturbed state the fluid in $x_2 < 0$ is at rest, whereas in $x_2 > 0$ there is a uniform mean flow at velocity U (> 0) in the positive direction of the x_1 axis. The steady motion is bounded by a vortex sheet in the plane of the slit. A uniform time-harmonic pressure perturbation $p_0 e^{-i\omega t}$ ($\omega > 0$) is applied to the slit in $x_2 > 0$ and it is required to determine the linearized approximation to the perturbed flow.

In doing this we shall assume (without loss of generality) that the sound speed c and the mean fluid density ρ_0 may be taken to be constant throughout the flow. Further, if $M = U/c$ is the Mach number of the mean flow, and $k = \omega/c$ is the acoustic wavenumber, we shall require that

$$M^2 \ll 1, \quad ks \ll 1, \tag{2.1}$$

so that the width of the slit is small compared with the wavelength of possible acoustic disturbances.

Let $Z(x_1)e^{-i\omega t}$ denote the displacement of the vortex sheet from $x_2 = 0$. The x_2-component $v_+e^{-i\omega t}$ of velocity just above the sheet (i.e. at $x_2 = +0$), is then given by

$$v_+ = (-i\omega + U\,\partial/\partial x_1)\,Z, \tag{2.2}$$

where here and henceforth the harmonic time-factor is suppressed. Note that the representation (2.2) of v_+ may be extended to the whole of the upper surface of the plate by taking $Z = 0$ for $|x_1| > s$. This is equivalent to assuming that flow separation downstream of the slot does *not* occur. The perturbation potential ϕ_+, say, in $x_2 > 0$ can be expressed in terms of v_+ by making use of the Green's function $G_+(\mathbf{x}, y_1)$ which satisfies the convected wave equation

$$\{(-ik + M\,\partial/\partial x_1)^2 - (\partial^2/\partial x_1^2 + \partial^2/\partial x_2^2)\}\,G_+(\mathbf{x}, y_1) = 0 \tag{2.3}$$

in $x_2 > 0$, and the condition

$$\partial G_+/\partial x_2 = \delta(x_1 - y_1) \quad \text{on} \quad x_2 = +0. \tag{2.4}$$

The function G_+ is the flow perturbation generated by a line source of unit strength on $x_2 = 0$ at $x_1 = y_1$, and it is uniquely defined only when conditions at large distances from the slit are specified. In §§ 3.4 we shall examine situations in which the basic configuration of figure 1 is coupled to additional flow-structure systems, and their detailed specification will then lead to the required unique form for G_+.

It follows from (2.4) that

$$\phi_+ = \int v_+(y_1)\,G_+(\mathbf{x}, y_1)\,dy_1, \tag{2.5}$$

where the integration extends over the upper surface of the plane and slit. In all cases to be considered in this paper it will transpire that $G_+(\mathbf{x}, y_1) \equiv G_+(x_1 - y_1, x_2)$, so that $\partial G_+/\partial x_1 \equiv -\partial G_+/\partial y_1$. Hence, using (2.2) in (2.5), integrating by parts and recalling that $Z(y_1) = 0$ for $|y_1| > s$, we find in $x_2 > 0$:

$$\phi_+ = (-i\omega + U\,\partial/\partial x_1)\int_{-s}^{s} Z(y_1)\,G_+(\mathbf{x}, y_1)\,dy_1. \tag{2.6}$$

The perturbation pressure p_+ associated with ϕ_+ is given by means of Bernoulli's equation in the form

$$p_+/\rho_0 = -(-i\omega + U\,\partial/\partial x_1)\,\phi_+, \tag{2.7}$$

which combines with (2.6) and the applied pressure p_0 to show that in $x_2 > 0$ the net perturbation pressure is just

$$p = -\rho_0(-i\omega + U\,\partial/\partial x_1)^2\int_{-s}^{s} Z(y_1)\,G_+(\mathbf{x}, y_1)\,dy_1 + p_0. \tag{2.8}$$

By means of a similar line of reasoning, it follows that in $x_2 < 0$ the perturbation pressure is given by

$$p = -\rho_0 \omega^2 \int_{-s}^{s} Z(y_1)\, G_-(\mathbf{x}, y_1)\, dy_1, \tag{2.9}$$

where $G_-(\mathbf{x}, y_1)$ satisfies the non-convected form of the wave equation (2.3) in $x_2 < 0$ (i.e. with M set equal to zero), and represents the potential due to a line source on $x_2 = -0$ at $x_1 = y_1$, so that

$$\partial G_-/\partial x_2 = -\delta(x_1 - y_1) \quad \text{on} \quad x_2 = -0. \tag{2.10}$$

The linearized equation governing the motion of the vortex sheet is obtained by applying the condition of continuity of pressure across the mean position $x_2 = 0$ of the sheet. Thus allowing $x_2 \to \pm 0$ in respectively equations (2.8), (2.9) we have for $|x_1| < s$:

$$\omega^2 \int_{-s}^{s} Z(y_1)\, G_-(x_1, -0, y_1)\, dy_1 - (-i\omega + U\,\partial/\partial x_1)^2 \int_{-s}^{s} Z(y_1)\, G(x_1, +0, y_1)\, dy_1 = -p_0/\rho_0. \tag{2.11}$$

Introducing the dimensionless variables

$$\xi = x_1/s, \quad \eta = y_1/s, \quad \zeta = Z/s, \tag{2.12}$$

and recalling the definition $\epsilon = \omega s/U$ of the reduced frequency given in § 1, we may also set (2.11) in the form

$$\epsilon^2 \int_{-1}^{1} \zeta(\eta)\, G_-(\xi, \eta)\, d\eta + (\epsilon + i\,\partial/\partial\xi)^2 \int_{-1}^{1} \zeta(\eta)\, G_+(\xi, \eta)\, d\eta = -p_0/\rho_0 U^2, \quad |\xi| < 1, \tag{2.13}$$

where an obvious abreviated notation for the arguments of the Green's functions has been adopted.

In §§ 3, 4 it will be shown that the condition (2.1) permits the Green's functions $G_\pm(\xi, \eta)$ to be expressed in a common approximate form when $|\xi|, |\eta| < 1$, namely:

$$\left.\begin{aligned} G_+(\xi, \eta) &= \pi^{-1} \ln|\xi - \eta| + a_+, \\ G_-(\xi, \eta) &= \pi^{-1} \ln|\xi - \eta| + a_-. \end{aligned}\right\} \tag{2.14}$$

The quantities a_+, a_- are complex constants, independent of ξ, η, which depend on the coupling of the motion in the slit to the particular flow-structure systems considered below in §§ 3, 4, where their explicit values will be calculated. Equation (2.13) accordingly becomes

$$[\epsilon^2 + (\epsilon + i\,\partial/\partial\xi)^2] \int_{-1}^{1} \zeta(\eta) \ln|\xi - \eta|\, d\eta = -\pi p_0/\rho_0 U^2 - \pi\epsilon^2(a_+ + a_-)\, q \quad (|\xi| < 1), \tag{2.15}$$

where q is the *flux* defined by

$$q = \int_{-1}^{1} \zeta(\eta)\, d\eta. \tag{2.16}$$

Equation (2.15) constitutes a second-order, linear differential equation which is satisfied by the integrated term within the interval $|\xi| < 1$. The inhomogeneous term on the right-hand side is independent of ξ, so that the solution may be written down immediately in the form:

$$\int_{-1}^{1} \zeta(\eta) \ln|\xi-\eta|\, d\eta = \chi(\xi) \quad (|\xi| < 1), \tag{2.17}$$

where

$$\chi(\xi) = C + \alpha\, e^{i\epsilon_1\xi} + \beta\, e^{i\epsilon_2\xi}, \tag{2.18}$$

C is the particular integral

$$C = -\tfrac{1}{2}\pi q(a_+ + a_-) - \pi p_0/2\rho_0\epsilon^2 U^2, \tag{2.19}$$

and α, β are arbitrary constants. The exponential terms on the right of (2.18) represent the general solution of the homogeneous differential equation, and the quantities ϵ_1, ϵ_2 are the roots X of the *auxiliary* equation $\epsilon^2 + (\epsilon - X)^2 = 0$, namely

$$\epsilon_1 = \epsilon(1+i), \quad \epsilon_2 = \epsilon(1-i). \tag{2.20}$$

These correspond respectively to exponentially decaying and growing disturbances on the vortex sheet (with increasing values of ξ), and are, in fact, precisely the eigenvalues which characterize the Kelvin–Helmholtz instability of an infinitely extended vortex sheet in incompressible flow.

The result (2.17) expresses a weighted distribution of the displacement of the vortex sheet as a constant term together with a linear combination of Kelvin–Helmholtz modes. This may be contrasted with the treatments of this and related problems due to Ronneberger (1972), Elder (1978), Tam & Block (1978) and Fletcher (1979), who assume that the displacement itself is equal to a linear combination of interfacial waves. These authors neglect the effect of the rigid boundaries on the motion of the sheet. Their influence may be understood by noting, for example from (2.6), (2.14) and (2.17), that the perturbation potential ϕ_+ just above the vortex sheet (on $x_2 = +0$) can also be represented in terms of a linear combination of Kelvin–Helmholtz modes, and similarly for the potential ϕ_-, say, on the lower surface of the sheet. This is because the rigid portions of the plate are hydrodynamically equivalent to distributions of surface forces – dipoles – which, in an ideal fluid, act in directions normal to the rigid surfaces. In consequence there is no contribution to the perturbation potentials at $x_2 = \pm 0$ within the slit, since this lies in a null direction of the surface dipoles. On the other hand, equation (2.2) relates the displacement Z of the vortex sheet to $v_+ = (\partial\phi_+/\partial x_2)_{x_2=0}$, and the value of the latter is determined by the details of the potential at points in $x_2 > 0$, where the contribution from the surface dipoles cannot be ignored. The analytical representation of the displacement must accordingly be expected to depend on the interaction of the vortex sheet with the plate.

Equation (2.17) is a singular integral equation for the displacement $\zeta(\xi)$, whose solution is given, for example, in Carrier, Krook & Pearson (1966, p. 428):

$$\zeta = \frac{1}{\pi^2(1-\xi^2)^{\frac{1}{2}}}\left\{ \int_{-1}^{1} \frac{(1-\eta^2)^{\frac{1}{2}}}{\eta-\xi} \chi'(\eta)\, d\eta - \frac{1}{\ln(2)} \int_{-1}^{1} \frac{\chi(\eta)\, d\eta}{(1-\eta^2)^{\frac{1}{2}}} \right\}, \tag{2.21}$$

where $\chi'(\eta) \equiv \partial\chi/\partial\eta$ and the first integral is a principal value. The values of the arbitrary constants α, β in the definition (2.18) of $\chi(\xi)$ must be determined by imposing two constraints on the solution (2.21). Since the displacement vanishes on the rigid surfaces, the obvious choice is to require that

$$\text{(I)} \qquad \zeta \to 0 \quad \text{as} \quad \xi \to \pm 1. \tag{2.22}$$

This will yield a solution ζ which varies continuously at both ends of the slit. Experiments indicate, however, that, although ζ is generally well behaved at the leading edge ($\xi = -1$) of the slit, on the contrary, the interaction of the vortex sheet with the trailing edge ($\xi = 1$) is far from smooth. One can argue that, in order to represent this interaction on the basis of linear theory, the displacement should be allowed to retain the singular, inverse square root, behaviour accorded by (2.21) as $\xi \to 1$. This will be the case if both of the disposable constants α, β are fixed by conditions imposed at the leading edge of the slit, which we shall take to be

$$\text{(II)} \qquad \zeta, \partial\zeta/\partial\xi \to 0 \quad \text{as} \quad \xi \to -1, \tag{2.23}$$

i.e. that the vortex sheet leaves the upstream edge tangentially in accordance with the Kutta condition. A second, and more significant, reason for preferring the Kutta condition (II) over case (I) is that case (II) involves the generation of additional vorticity at the leading edge in order to maintain the smooth flow there, and it is only by this means that an exchange of energy between the mean and the unsteady slit flows can be effected. We shall see below that no transfer of energy occurs in case (I).

Consider first the Kutta condition case (II). Substitute from (2.18) into (2.21) and perform the integrations with the aid of the definition (Gradshteyn & Ryzhik 1965, p. 973) of the generating function of the Bessel coefficients $J_n(z)$ to obtain

$$\zeta(\xi) = \frac{-1}{\pi(1-\xi^2)^{\frac{1}{2}}}\Big\{[C+\alpha J_0(\epsilon_1)+\beta J_0(\epsilon_2)]/\ln(2) + i\epsilon_1\alpha[\xi J_0(\epsilon_1)+iJ_1(\epsilon_1)]$$
$$+ i\epsilon_2\beta[\xi J_0(\epsilon_2)+iJ_1(\epsilon_2)] - 2\pi i \sum_{n=1}^{\infty} i^n \sin\vartheta \sin(n\vartheta)\,[\alpha\epsilon_1 J_n(\epsilon_1)+\beta\epsilon_2 J_n(\epsilon_2)]\Big\}, \tag{2.24}$$

where $\vartheta = \cos^{-1}\xi$.

Condition (2.23) provides two relations for the determination of the coefficients α, β. The constant C in (2.24) depends, however, on the unknown flux q through the definition (2.19). A third equation for the determination of q is obtained by integrating (2.24) over the slit ($|\xi| < 1$) and using (2.16). Actually it is simpler to start from the formal expression (2.21) and to observe that the principal-value integral makes no contribution to q. In this way we find

$$q = \frac{-1}{\ln(2)}\{C+\alpha J_0(\epsilon_1)+\beta J_0(\epsilon_2)\}. \tag{2.25}$$

The relations obtained from the Kutta condition (2.23) are

$$q + i\epsilon_1\alpha[J_0(\epsilon_1)-iJ_1(\epsilon_1)] + i\epsilon_2\beta[J_0(\epsilon_2)-iJ_1(\epsilon_2)] = 0, \tag{2.26}$$

$$\alpha\epsilon_1\{J_0(\epsilon_1)-2i\epsilon_1[J_0(\epsilon_1)-iJ_1(\epsilon_1)]\} + \beta\epsilon_2\{J_0(\epsilon_2)-2i\epsilon_2[J_0(\epsilon_2)-iJ_1(\epsilon_2)]\} = 0, \tag{2.27}$$

where use has been made of the recurrence relation $2nJ_n(z) = z[J_{n-1}(z)+J_{n+1}(z)]$ (Gradshteyn & Ryzhik 1965, p. 967) in obtaining (2.27).

The system (2.25)–(2.27), together with the definition (2.19) of C, determines the

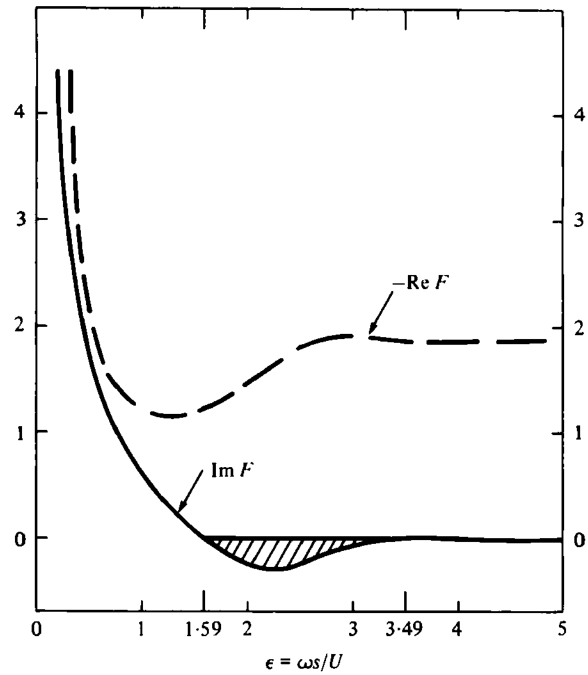

FIGURE 2. Variation of the real and imaginary parts of $F(\epsilon)$ defined in (2.29) as a function of the reduced frequency $\epsilon = \omega s/U$.

parameters α, β, q in terms of the applied pressure p_0. It will be sufficient to quote the result for the flux q, which we shall express in the form

$$q\{F(\epsilon)+\ln(2)-\tfrac{1}{2}\pi(a_+ + a_-)\} = \pi p_0/2\rho_0\epsilon^2U^2, \tag{2.28}$$

where the complex-valued function $F(\epsilon)$ is given by

$$F(\epsilon) = \frac{(4\epsilon+i)\,|J_0(\epsilon_1)|^2 - 2i\epsilon\{J_0(\epsilon_1)\,J_1(\epsilon_2)+J_0(\epsilon_2)\,J_1(\epsilon_1)\}}{\epsilon\{J_0(\epsilon_2)\,J_1(\epsilon_1)-J_0(\epsilon_1)\,J_1(\epsilon_2)-4i\epsilon[J_0(\epsilon_1)-iJ_1(\epsilon_1)]\,[J_0(\epsilon_2)-iJ_1(\epsilon_2)]\}}. \tag{2.29}$$

In problems where there is no externally applied pressure perturbation p_0, so that the right-hand side of (2.28) vanishes, the zeros ϵ (if any) of the expression in the curly brackets on the left of (2.28) represent the natural (unforced) oscillations of the system.

It will be demonstrated subsequently that there can be a transfer of energy from the mean flow to the aperture oscillations only if the imaginary part of $F(\epsilon)$ is *negative*. The dependence of the real and imaginary parts of $F(\epsilon)$ on real values of the reduced frequency $\epsilon = \omega s/U$ is depicted in figure 2. The following general points may be noted:

$$\left.\begin{array}{ll}\text{(i)} & F(\epsilon) \simeq \dfrac{-1}{3\epsilon^2}\left\{1-\dfrac{8i\epsilon}{3}\right\} \quad \text{as} \quad \epsilon \to 0, \\ \text{(ii)} & F(\epsilon) \simeq -2 \quad \text{as} \quad \epsilon \to \infty.\end{array}\right\} \tag{2.30}$$

(iii) The principal range in which $\mathrm{Im}(F) < 0$ (cross-hatched in the figure) is $1{\cdot}59 < \epsilon < 3{\cdot}49$, and $\mathrm{Im}(F)$ attains a minimum value of $-0{\cdot}31$ at $\epsilon \simeq 2{\cdot}30$. Although $\mathrm{Im}(F)$ does assume negative values for $\epsilon > 3{\cdot}49$, it always exceeds $-0{\cdot}014$, and such values will not be significant in the present discussion. These characteristics may also

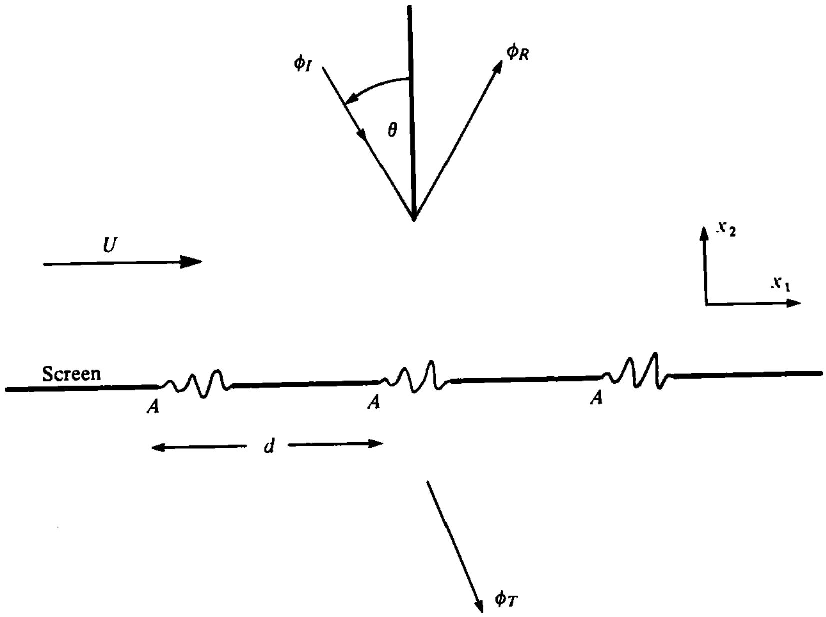

FIGURE 3. Diffraction of sound by a perforated screen in the presence of a uniform mean flow in $x_2 > 0$.

be expressed in the following descriptive manner: Let $\lambda = 2\pi s/\epsilon$ denote the hydrodynamic wavelength of the disturbance on the vortex sheet; then, since $1{\cdot}59 \simeq \frac{1}{2}\pi$, we can say that Im (F) is negative when the width $2s$ of the slit satisfies

$$\tfrac{1}{2}\lambda < 2s < 1{\cdot}1\lambda, \tag{2.31}$$

and, moreover, Im (F) assumes its greatest negative value when $2s \simeq 3\lambda/4$.

Finally, consider the corresponding results for case (I) of (2.22), in which the displacement ζ is assumed to vary continuously at both ends of the slit. Proceeding in the manner described above, one again obtains a defining equation (2.28) for the flux q, except that $F(\epsilon)$ given above by (2.29) must be replaced by $F_I(\epsilon)$, say, where

$$F_I(\epsilon) = \frac{|J_0(\epsilon_1)|^2}{[J_0(\epsilon_1)\,J_1(\epsilon_2) - J_0(\epsilon_2)\,J_1(\epsilon_1)]}\left(\frac{1}{\epsilon_1} - \frac{1}{\epsilon_2}\right). \tag{2.32}$$

Since equations (2.20) show that the eigenvalues ϵ_1, ϵ_2 are complex conjugates, it follows that $F_I(\epsilon)$ is *real* for real ϵ and, as we shall see, this implies that there can be no exchange of energy between the mean and unsteady components of the flow.

3. The effect of mean shear on acoustical diffraction by a perforated screen

Our first application of the above analysis is to the diffraction problem illustrated in figure 3. A plane sound wave of angular frequency $\omega > 0$ is incident from $x_2 > 0$ on a thin rigid screen which occupies $x_2 = 0$ and is perforated with parallel, equal and equidistant slits each of width $2s$ and orientated as in § 2. The distance between the centre-lines of adjacent slits is denoted by d. As before, there exists a low-Mach-number mean flow at speed U in the x_1 direction in $x_2 > 0$, and no mean flow in $x_2 < 0$; the sound speed and mean density are taken to be uniform throughout the fluid.

Let Φ_I be the potential of the incident wave, and assume that the wave propagates parallel to the (x_1, x_2) plane. It therefore satisfies the convected wave equation (2.3), and will be taken in the elementary exponential form

$$\Phi_I(\mathbf{x}) = \exp\left\{\frac{ik}{(1+M\sin\theta)}(x_1\sin\theta - x_2\cos\theta)\right\}, \tag{3.1}$$

where k, M are respectively the acoustic wavenumber and mean-flow Mach number introduced in § 2. The angle θ in (3.1) is the angle between the acoustic wavenormal and the x_2 axis (see figure 3); in general it does not coincide with the direction of acoustic energy propagation in the moving medium. The factor $(1+M\sin\theta)$ accounts for the Doppler shift in the wavelength which occurs with different directions of propagation when the frequency ω is constant and measured in a frame fixed relative to the screen.

In addition to (2.1) it is assumed that $kd \ll 1$ (acoustic wavelength large compared with the spacing of the slits). It follows, in particular, that at large distances from the screen the diffracted sound reduces to specularly reflected and transmitted waves, Φ_R, Φ_T respectively, which are given in terms of reflection and transmission coefficients R, T, say, by

$$\left.\begin{aligned} \Phi_R &= R\exp\left\{\frac{ik}{(1+M\sin\theta)}(x_1\sin\theta + x_2\cos\theta)\right\}, \\ \Phi_T &= T\exp\left\{\frac{ik}{(1+M\sin\theta)}(x_1\sin\theta - x_2[(1+M\sin\theta)^2 - \sin^2\theta]^{\frac{1}{2}})\right\}. \end{aligned}\right\} \tag{3.2}$$

The square root in the argument of the exponential of the transmitted wave is positive imaginary when the angle of incidence is negative (incident wave propagating against the mean flow) and

$$-\tfrac{1}{2}\pi < \theta < -\sin^{-1}(1/(1+M)); \tag{3.3}$$

in this case Φ_T decays exponentially as $x_2 \to -\infty$.

Take the origin of co-ordinates in the centre of the slit designated by A_0, say, and let q be the dimensionless flux through A_0 defined as in (2.16). The reflection and transmission coefficients can be expressed in terms of q in the manner described by Howe (1980*a*) for the analogous problem involving uniform mean flow on *both* sides of the screen. We find, in fact,

$$T = \omega s^2 q/d\bar{n}_2, \quad R = 1 - \omega s^2 q/dn_2, \tag{3.4}$$

where

$$\left.\begin{aligned} n_2 &= k\cos\theta/(1+M\sin\theta), \\ \bar{n}_2 &= k\{(1+M\sin\theta)^2 - \sin^2\theta\}^{\frac{1}{2}}/(1+M\sin\theta). \end{aligned}\right\} \tag{3.5}$$

The flux q can be calculated from equation (2.28) when the coefficients a_+, a_-, which define the local forms (2.14) of the Green's functions $G_\pm(\mathbf{x}, y_1)$, are known. The latter are given by Howe (1980*a*), from which we deduce that

$$\left.\begin{aligned} a_+ &= -i/dn_2 + \pi^{-1}\ln(2\pi s/d), \\ a_- &= -i/d\bar{n}_2 + \pi^{-1}\ln(2\pi s/d), \end{aligned}\right\} \tag{3.6}$$

provided that the angle of incidence θ is *outside* of the range (3.3) of total reflection. When (3.3) is satisfied the term $-i/d\bar{n}_2$ in the second of (3.6) is omitted.

To complete the determination of q from (2.28) it remains to specify the pressure p_0 applied to the upper surface of the screen at A_0. It is equal to the pressure which obtains when the slits are absent, and at small mean-flow Mach numbers and long acoustic wavelengths we have, from Bernoulli's equation,

$$p_0 = 2i\omega\rho_0\Phi_I(0). \tag{3.7}$$

The factor of 2 in (3.7) arises from the specular reflection, with $R = 1$, which occurs in the absence of slits.

Substituting from (3.6), (3.7) into equation (2.28), and using the results (3.4), we finally obtain:

$$\left.\begin{aligned} T &= \frac{\pi i}{\bar{n}_2 d}\Big/\left\{\frac{\pi i}{2d}\left(\frac{1}{n_2}+\frac{1}{\bar{n}_2}\right)+\ln(2/\pi\sigma)+F(\epsilon)\right\}, \\ R &= 1-\frac{\pi i}{n_2 d}\Big/\left\{\frac{\pi i}{2d}\left(\frac{1}{n_2}+\frac{1}{\bar{n}_2}\right)+\ln(2/\pi\sigma)+F(\epsilon)\right\}, \end{aligned}\right\} \tag{3.8}$$

in which

$$\sigma = 2s/d \tag{3.9}$$

is the *open area ratio* of the screen. When total reflection occurs we take $T = 0$.

To interpret these formulae we proceed to examine the acoustic energy balance. The mean acoustic power flux in the i-direction is equal to $\langle\rho v_i h\rangle$, where v_i is the i-component of velocity, ρ, h are respectively the density and total enthalpy of the fluid, and the angle brackets denote an average over a wave period (Landau & Lifshitz 1959, §§6 and 64). In isentropic flow we can take $h = \mathrm{Re}\{i\omega\Phi e^{-i\omega t}\}$. It follows that, if Π_I is the acoustic power incident on the screen, and Π_S is the total reflected and transmitted powers, then

$$\Pi_S/\Pi_I = \frac{\bar{n}_2|T|^2+n_2|R|^2}{n_2} \tag{3.10}$$

(cf. Howe 1980*a*, equation (4.7)). Equations (3.8) may be used to express this in the form

$$\frac{\Pi_S}{\Pi_I} = 1-\frac{(2\pi/n_2 d)\,\mathrm{Im}\,(F(\epsilon))}{\left|\dfrac{\pi i}{2d}\left(\dfrac{1}{n_2}+\dfrac{1}{\bar{n}_2}\right)+\ln(2/\pi\sigma)+F(\epsilon)\right|^2}, \tag{3.11}$$

where $1/\bar{n}_2$ is omitted at total reflection.

Acoustic energy is therefore seen to be conserved provided that $F(\epsilon)$ is real. This implies that, for the first of the two cases considered in §2 (case (I)) in which the displacement of the vortex sheet in a slit tends continuously to zero at both ends, and for which $F(\epsilon)$ is equal to the real-valued function $F_I(\epsilon)$ defined in (2.32), acoustic energy is conserved during diffraction at the screen. In case (II), however, where the Kutta condition is applied, and the motion of the vortex sheet is discontinuous and singular at the trailing edge, it is seen by reference to figure 2 that the net acoustic energy can increase or decrease during the interaction with the screen. Indeed, noting that n_2 is a positive quantity, it follows from the discussion at the end of §2 that the acoustic field is attenuated if $\omega s/U < \frac{1}{2}\pi$, and enhanced if $\frac{1}{2}\pi < \omega s/U < 3{\cdot}49$. Energy is conserved for higher values of the reduced frequency.

Perforated screens in a grazing mean flow have been used to attenuate undesirable reverberant sound fields in, for example, the heat exchanger cavity of a nuclear reactor. The mean flow Mach numbers involved are always small, and the open area ratio σ rarely exceeds 0·1. The present theory assumes that kd is small, say less than 0·5, and this is generally compatible with the practical situation so that, since $\epsilon \equiv kd\sigma/2M$, it is clear that, except for exceptionally small values of M, the reduced frequency is likely to be very much less than unity. This places us in the region of figure 2 for which acoustic energy is ***dissipated***.

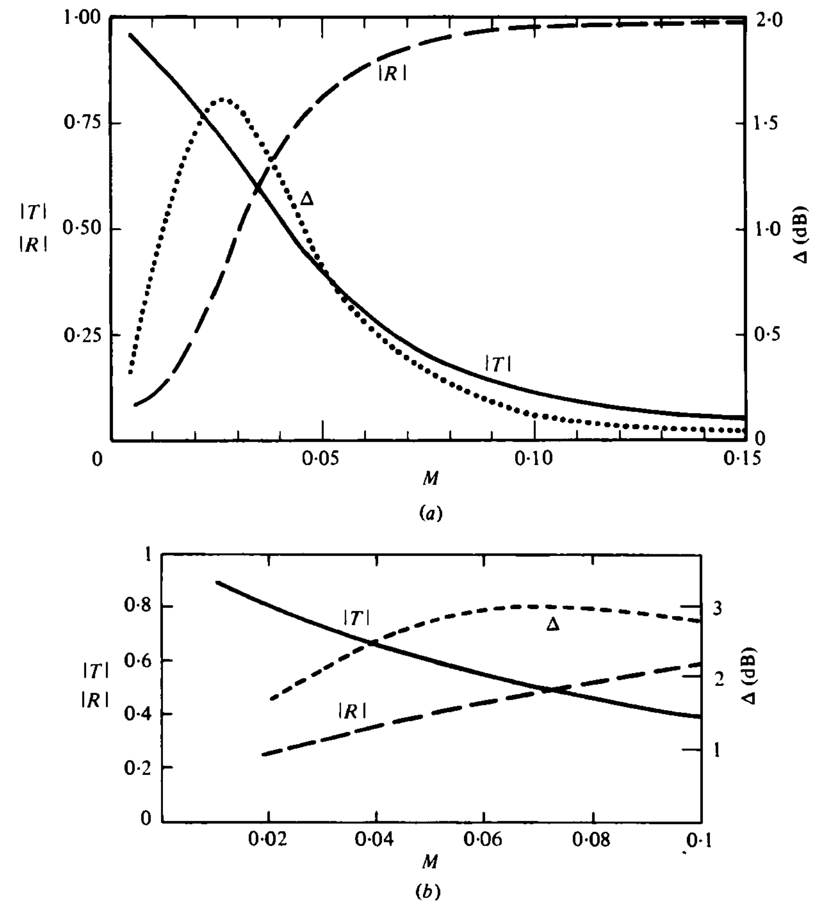

FIGURE 4. Variation of $|T|$, $|R|$ and Δ (a) with the mean-flow Mach number M in $x_2 > 0$, (b) with the mean flow on both sides of the screen (after Howe 1980a). The sound is incident normally on the screen, and $kd = 0{\cdot}2$, $\sigma = 0{\cdot}05$.

For the remainder of this section we shall confine attention to the Kutta condition (case (II)) model of the unsteady motion in the slits. The theoretical predictions will be illustrated for a sound wave at normal incidence ($\theta = 0$), for which equations (3.8), (3.10) reduce to

$$\left.\begin{aligned} T = 1 - R &= 1\bigg/\left\{1 - \frac{2iM\epsilon}{\pi\sigma}(\ln(2/\pi\sigma) + F(\epsilon))\right\}, \\ \Pi_S/\Pi_I &= |R|^2 + |T|^2, \end{aligned}\right\} \tag{3.12}$$

in which it may be noted that $2M\epsilon/\sigma \equiv kd$.

Figure 4 (*a*) presents the dependence of $|T|$, $|R|$ on the mean flow Mach number M when $kd = 0{\cdot}2$ and the open area ratio $\sigma = 0{\cdot}05$. Acoustic energy is always dissipated in this case unless M is smaller than 0·0032. As the Mach number increases, $|T|$, $|R|$ rapidly assume their respective asymptotic values of zero and unity predicted by (3.12) as $\epsilon \to 0$ (cf. the first of equations (2.30)). This behaviour may be contrasted with the situation in the absence of flow (first treated by Rayleigh 1897), obtained by discarding the dependence on $F(\epsilon)$ in our results, for which $|T| \simeq 0{\cdot}9871$, $|R| \simeq 0{\cdot}1599$. Here acoustic energy is conserved, of course, and more than 97 % of the incident energy is transmitted by the screen! On the contrary, as the reduced frequency $\omega s/U \to 0$ in the presence of mean shear, *all* of the incident acoustic energy is reflected. For the case illustrated in figure 4 (*a*), ϵ is equal to 0·03, and $|T| = 0{\cdot}0521$ when $M = 0{\cdot}15$, and less than 0·3 % of the energy is transmitted.

The attenuation experienced by the sound is measured on a decibel scale by means of the absorption coefficient Δ, defined by

$$\Delta = -10\log_{10}(\Pi_S/\Pi_I). \tag{3.13}$$

The dotted curve in figure 4(*a*) depicts the variation of Δ with M, from which the maximum attenuation is seen to occur at $M \simeq 0{\cdot}027$, where $\Delta \simeq 1{\cdot}5$ dB.

These predictions may be compared with the results obtained by Howe (1980*a*) when the mean flow is the same on both sides of the screen, and for which attenuation occurs at all frequencies. The corresponding predicted variations of $|T|$, $|R|$, Δ in this case are shown in figure 4 (*b*). The moduli $|T|$, $|R|$ are seen to vary more slowly with increasing M. The maximum value of Δ is greater, however; as much as 50 % of the incident sound power is absorbed when $M \simeq 0{\cdot}07$. In fact, Howe shows that to a good approximation the maximum attenuation at normal incidence is just over 3 dB and occurs when

$$M \simeq \tfrac{1}{2}\pi\sigma. \tag{3.14}$$

In the presence of mean shear the magnitude of the maximum attenuation depends critically on the frequency of the sound, and there is no simple relation analogous to (3.14). For a given value of kd, however, one can calculate the value of M/σ for which Δ is a maximum, and demonstrate the relative insensitivity of the results to variations of the open area ratio in the range $0{\cdot}01 \leqslant \sigma \leqslant 0{\cdot}05$. Figure 5 shows the dependence of M/σ and the corresponding optimal attenuation Δ on values of kd in (0, 0·5) for normal incidence. In no case does the attenuation attain a value approaching the 3 dB optimum for uniform mean flow.

In figure 6 the dependencies of $|T|$, $|R|$, Δ on the reduced frequency ϵ are illustrated for normal incidence, $\sigma = 0{\cdot}05$, and for a constant mean-flow Mach number $M = 0{\cdot}015$. The theory is of doubtful validity for $\epsilon > 1{\cdot}7$, for which kd exceeds unity, but the results should still be qualitatively correct, and indicate that the acoustic field experiences *negative damping* in the range $\frac{1}{2}\pi < \epsilon < 3{\cdot}49$. The additional energy acquired by the sound must be extracted from the mean flow, and the enhancement peaks at $\epsilon = 2{\cdot}3 \simeq \frac{3}{4}\pi$ where the modulus of the transmission coefficient exceeds unity and when each slit in the screen is occupied by approximately three quarters of a hydrodynamic wavelength of the disturbed motion of the vortex sheet.

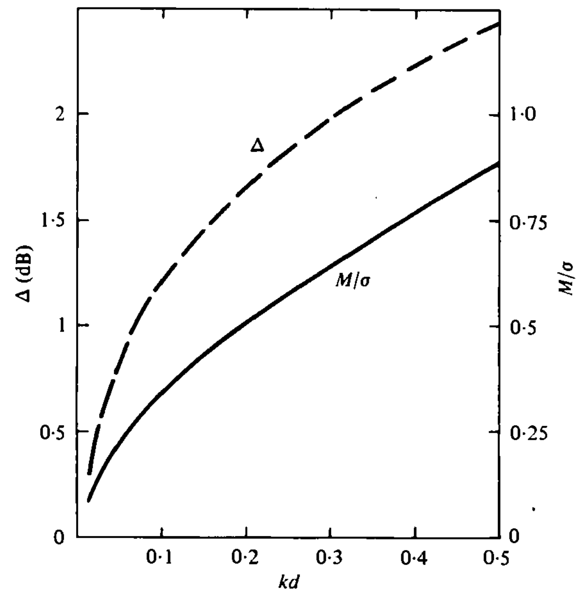

FIGURE 5. Variation with kd of the optimal value of M/σ yielding the maximal attenuation Δ. The case shown is for normal incidence and for $0{\cdot}01 \leqslant \sigma \leqslant 0{\cdot}05$.

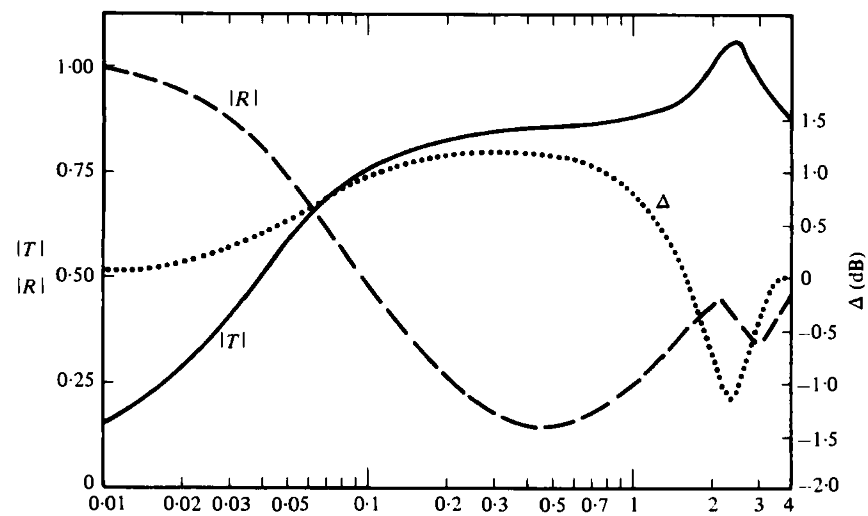

FIGURE 6. Variation of $|T|$, $|R|$, Δ with the reduced frequency ϵ for normal incidence and $M = 0{\cdot}015$, $\sigma = 0{\cdot}05$.

4. The excitation of wall-cavity oscillations

The theory of § 2 is now applied to model the generation of self-sustained oscillations by a nominally steady flow over a cavity in a plane wall. Only the simplified geometrical configuration illustrated in figure 7 will be discussed, although the analytical details are easily modified to deal with more complicated cavity interiors. The cavity consists of a rigid-walled, rectangular parallelepiped whose sides are parallel to the co-ordinate axes and respectively of lengths (h, l, d). The cavity communicates with a uniform external mean flow at speed U in the positive x_1 direction through a narrow, symmetrically located slit of width $2s$ and length d which spans the transverse dimension of the cavity. The origin of co-ordinates is taken in the centre of the slit, as in § 2, and the upper wall of the cavity (in $x_2 = 0$) is assumed to have negligible thickness. We shall further suppose that

$$2s \ll d, h \ll l, \tag{4.1}$$

so that the lower-order acoustic resonances are 'depth' modes which have no dependence on x_1 and x_3.

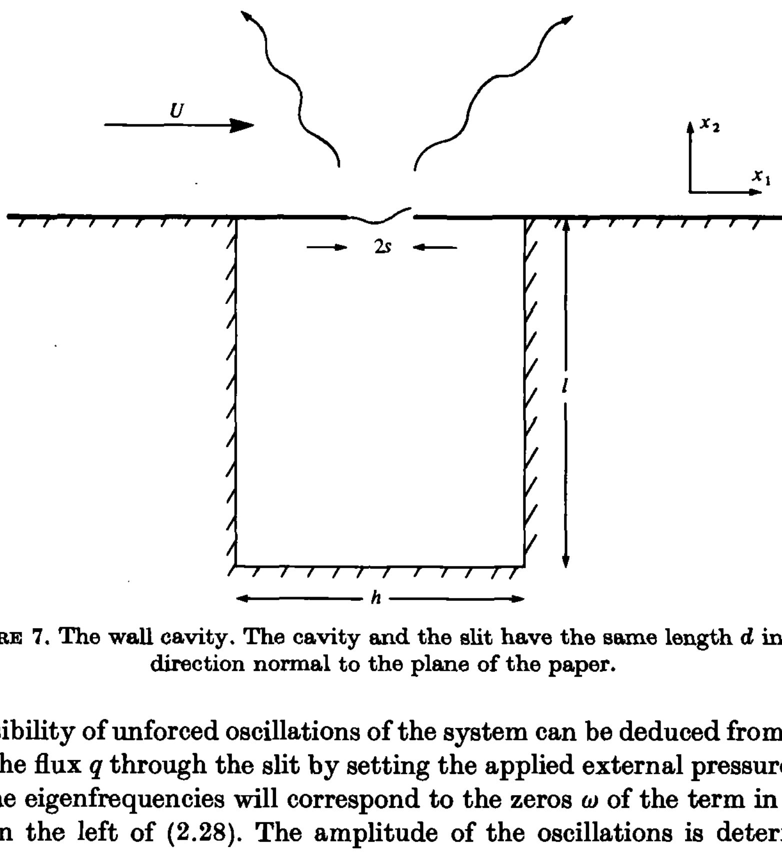

FIGURE 7. The wall cavity. The cavity and the slit have the same length d in the direction normal to the plane of the paper.

The possibility of unforced oscillations of the system can be deduced from equation (2.28) for the flux q through the slit by setting the applied external pressure p_0 equal to zero. The eigenfrequencies will correspond to the zeros ω of the term in the curly brackets on the left of (2.28). The amplitude of the oscillations is determined by nonlinear aspects of the unsteady flow in the slit, and cannot, therefore, be predicted by the present linear theory.

In order to make use of (2.28) it is first necessary to calculate the coefficients a_+, a_- which define the near-field approximations (2.14) to the Green's functions $G_\pm(\mathbf{x}, y_1)$. Since the aspect ratio $d/2s$ of the slit is large, we shall neglect end effects and assume that in the immediate vicinity of the slit the motion is two-dimensional, in planes parallel to the (x, x_2) plane.

Consider first $G_-(\mathbf{x}, y_1)$, which characterizes the two-dimensional motion in the cavity. For the lower-order resonances the acoustic wavelengths are comparable to the vertical dimension l of the cavity. In the body of the cavity the motion consists of plane compressional modes, and we can write

$$G_-(\mathbf{x}, y_1) \simeq A \cos\{k(x_2+l)\}. \tag{4.2}$$

This is a solution of the non-convected wave equation and satisfies $\partial G_-/\partial x_2 = 0$ at the lower end $x_2 = -l$. The coefficient A is determined from the line source condition (2.10) which is to be imposed on the upper wall of the cavity. Since the wavelengths are large relative to h, the motion near the upper end will approximate that of an incompressible fluid, and when y_1 lies within the slit, so that

$$|y_1| < s \ll h,$$

the form of $G_-(\mathbf{x}, y_1)$ can be calculated from the corresponding potential for a line source at the *origin*, i.e. near the upper end of the cavity

$$G_-(\mathbf{x}, y_1) = B + \mathrm{Re}\left\{\frac{1}{\pi}\ln\left[\sinh\left(\pi z/h\right)\right]\right\} + O(s/h) \quad (|y_1| < s), \tag{4.3}$$

where $z = x_2 + i(x_1 - y_1)$ and B is constant (Milne-Thomson 1968, § 10.5).

The values of the coefficients A, B are obtained by equating these different expressions (4.2), (4.3) for G_- within a common region of validity defined by

$$h \ll |x_2| \ll 1/k. \tag{4.4}$$

This gives

$$\left.\begin{aligned} B - \pi^{-1}\ln(2) &= A\cos(kl), \\ \frac{1}{h} &= Ak\sin(kl), \end{aligned}\right\} \tag{4.5}$$

so that

$$\left.\begin{aligned} A &= 1/kh\sin(kl), \\ B &= \ln(2)/\pi + \cot(kl)/kh. \end{aligned}\right\} \tag{4.6}$$

Using the second of (4.6) in (4.3), and assuming that $\mathbf{x}$, y_1 both lie within the slit ($x_2 = -0, |x_1 - y_1| < 2s \ll h$), we find

$$G_-(x_1, 0, y_1) \simeq \cot(kl)/kh + \pi^{-1}\ln|2\pi(x_1 - y_1)/h|. \tag{4.7}$$

When this result is expressed in terms of the dimensionless variables ξ, η we see, by comparison with (2.14), that

$$a_- = \pi^{-1}\ln(2\pi s/h) + \cot(kl)/kh. \tag{4.8}$$

The calculation of G_+ must take account of the spherical spreading of sound waves emitted by the slit, and we therefore start by considering the three-dimensional Green's function $\mathscr{G}_+$, say, which satisfies

$$\{(-ik + M\,\partial/\partial x_1)^2 - (\partial^2/\partial x_1^2 + \partial^2/\partial x_2^2 + \partial^2/\partial x_3^2)\}\,\mathscr{G}_+ = 0 \quad (x_2 > 0), \tag{4.9}$$

with

$$\partial\mathscr{G}_+/\partial x_2 = \delta(x_1 - y_1)\,\delta(x_3 - y_3) \quad (x_2 = +0). \tag{4.10}$$

When M^2 can be neglected relative to unity we have

$$\mathscr{G}_+(\mathbf{x}, y_1, y_3) = \frac{-1}{2\pi\,|\mathbf{x}-\mathbf{y}|}\exp\left[ik\{|\mathbf{x}-\mathbf{y}| - M(x_1-y_1)\}\right], \tag{4.11}$$

in which $\mathbf{x} = (x_1, x_2, x_3)$, $\mathbf{y} = (y_1, y_3)$. This is used to calculate the potential ϕ_+ by means of

$$\phi_+ = \iint v_+(y_1)\,\mathscr{G}_+(\mathbf{x}, y_1, y_3)\,dy_1\,dy_3. \tag{4.12}$$

The assumption of two-dimensional flow in the slit implies that v_+, ϕ_+ are independent of the transverse co-ordinate x_3. When $\mathbf{x}$ lies within the slit, however, ϕ_+ will, according to (4.12), exhibit a weak dependence on x_3 which is associated with the effects of the ends of the slit. We shall formally remove this by averaging (4.12) over the interval $-\frac{1}{2}d < x_3 < \frac{1}{2}d$ occupied by the slit. This procedure is tantamount to defining the value of the two-dimensional Green's function of § 2 by

$$G_+(x_1, 0, y_1) = \frac{1}{d}\int_{-\frac{1}{2}d}^{\frac{1}{2}d}\int_{-\frac{1}{2}d}^{\frac{1}{2}d}\mathscr{G}_+(x_1, 0, x_3, y_1, y_3)\,dy_3\,dx_3. \tag{4.13}$$

The relevant acoustic wavelengths are large compared with the transverse dimension d, so that in evaluating this integral for small $|x_1-y_1|$ we can make use of the approximation

$$\mathscr{G}_+(\mathbf{x}, y_1, y_3) \simeq -1/2\pi\,|\mathbf{x}-\mathbf{y}| - ik/2\pi. \tag{4.14}$$

in which case the definition (4.13) yields

$$G_+(x_1, 0, y_1) = -\frac{ikd}{2\pi} - \frac{1}{\pi}\left\{\sinh^{-1}(d/|x_1-y_1|) + \frac{|x_1-y_1|}{d}\left(1-\cosh\left[\sinh^{-1}(d/|x_1-y_1|)\right]\right)\right\}. \tag{4.15}$$

Now $\sinh^{-1}(d/|x_1-y_1|) \simeq \ln(2d/|x_1-y_1|)$ when x_1, y_1 both lie within the slit. Hence, introducing this approximation into (4.15), and comparing the result with (2.14), we finally conclude that

$$a_+ = \pi^{-1}\ln(se/2d) - ikd/2\pi, \tag{4.16}$$

where $e = 2{\cdot}71828\ldots$ is the base of the natural logarithm. Note that uncertainties in the averaging procedure used above can affect only the *real* part of a_+, and this will be seen below to influence the precise values of the resonance frequencies of the cavity, but to make no significant modification to predictions regarding the spontaneous excitation and suppression of the resonances.

The expressions (4.8), (4.16) for the coefficients a_-, a_+ are now substituted into the curly brackets of (2.28) and the result equated to zero to give the following equation whose roots determine the natural frequencies of the coupled cavity/mean flow system

$$\cot(kl) = 2kh\pi^{-1}\{\tfrac{1}{2}\ln(4hd/\pi e s^2) + \tfrac{1}{4}ikd + F(\epsilon)\}, \tag{4.17}$$

in which, we recall, $k = \omega/c$ and $\epsilon = \omega s/U$.

The relevant acoustic wavelengths are, by hypothesis, large compared with the dimensions h, d of the cavity, so that, in particular, $kh \ll 1$. Equation (4.17) may therefore be set in the approximate form

$$\cos\{kl+f(\omega)\} = 0, \tag{4.18}$$

where

$$f(\omega) = 2kh\pi^{-1}\{\tfrac{1}{2}\ln(4hd/\pi e s^2)+\tfrac{1}{4}ikd+F(\epsilon)\} \ll 1. \tag{4.19}$$

A first approximation to the solution of (4.18) is accordingly

$$\omega_n = \omega_n^0 - cf(\omega_n^0)/l \quad (n = 1, 2, \ldots), \tag{4.20}$$

where

$$\omega_n^0 = (n-\tfrac{1}{2})\pi c/l. \tag{4.21}$$

Equation (4.19) shows that $f(\omega)$ is in general a complex-valued function; it follows from the harmonic dependence $e^{-i\omega t}$ on the time, that small oscillations of the system will decay or grow according as $\mathrm{Im}(f) \gtrless 0$. Hence the spontaneous initiation of oscillations of frequency ω_n^0 will be possible provided that

$$\mathrm{Im}(f(\omega_n^0)) < 0. \tag{4.22}$$

Inspection of (4.19) indicates that there are two physically distinct contributions to $\mathrm{Im}(f)$: the first is provided by the second term in the curly brackets of (4.19) and accounts for energy losses from the oscillating system due to radiation into the ambient medium. The second is associated with $F(\epsilon)$, and depends on the interaction of the vortex sheet with the slit. Of the two models (cases (I), (II)) discussed in § 2, it has been shown that $F(\epsilon)$ assumes complex values only for the Kutta condition case (II). Thus the singular behaviour of the vortex sheet at the trailing edge of the slit predicted by the theory in case (II) appears to be an essential ingredient of a proper modelling of the cavity oscillations.

Before proceeding to a more quantitative discussion we shall introduce a correction to (4.20) which arises from the inclusion of dissipation due to viscous and thermal effects at the walls of the cavity. For depth modes this requires the addition to the right-hand side of (4.20) of a purely imaginary term which is equal to

$$-i\left(\frac{1}{d}+\frac{1}{h}\right)(\tfrac{1}{2}\omega_n^0)^{\frac{1}{2}}\{\nu^{\frac{1}{2}}+(\gamma-1)\chi^{\frac{1}{2}}\},$$

where ν, χ are respectively the kinematic viscosity and the thermometric conductivity of the fluid, and γ is the ratio of specific heats (see, for example, Landau & Lifshitz 1959, § 77). Condition (4.22) for the excitation of oscillations may now be expressed in the modified form

$$\mathrm{Im}\{-F(\epsilon_n)\} > \tfrac{1}{4}\pi(n-\tfrac{1}{2})\frac{d}{l}+\frac{1}{2}\left(\frac{l}{h}\right)^2\left(\frac{h}{d}+1\right)\left(\frac{\pi}{(2n-1)lc}\right)^{\frac{1}{2}}[\nu^{\frac{1}{2}}+(\gamma-1)\chi^{\frac{1}{2}}], \tag{4.23}$$

where $\epsilon_n = \omega_n^0 s/U$. The imaginary part of $F(\epsilon_n)$ must be negative and exceed in magnitude the sum of the terms on the right of (4.23) which respectively correspond to dissipation due to radiation and boundary-layer damping. Recalling the properties of $F(\epsilon)$ summarized at the end of § 2 and illustrated in figure 2, we see that self-sustained

n	Right-hand side of (4.25)	U_{min} (m s^{-1})	U_{max} (m s^{-1})
1	0·104	6·36	10·45
2	0·250	20·99	27·32

TABLE 1

oscillations are possible only if $1{\cdot}59 < \omega_n^0 s/U < 3{\cdot}49$ where $\mathrm{Im}(F) < 0$. This occurs for mean-flow velocities U lying in the range

$$0{\cdot}29\omega_n^0 s < U < 0{\cdot}63\omega_n^0 s. \tag{4.24}$$

Of course, the actual interval is smaller than this because $\mathrm{Im}(-F)$ must exceed the terms on the right of (4.23), and if the damping is large enough (specifically, if the right of (4.23) exceeds about 0·31), the theory predicts that oscillations are damped out for all values of ω and U.

By way of illustration, consider a cavity of depth $l = 30$ cm which has a slit of width $2s = 2$ cm, and let $d = h = 0{\cdot}2l$. In air we take $\nu = 0{\cdot}15\,\mathrm{cm^2\,s^{-1}}$, $\chi = 0{\cdot}21\,\mathrm{cm^2\,s^{-1}}$, $\gamma = 1{\cdot}4$. The inequality (4.23) becomes

$$\mathrm{Im}\{-F(\epsilon_n)\} > 0{\cdot}157(n-\tfrac{1}{2})\{1+0{\cdot}113/(n-\tfrac{1}{2})^{\frac{3}{2}}\} \quad (n = 1, 2, 3, \ldots), \tag{4.25}$$

from which we deduce that self-sustained oscillations are possible for $n = 1, 2$ only. For $n = 3$ the right-hand side of (4.25) is equal to 0·40. The approximate range of velocities $U_{min} < U < U_{max}$ over which excitation is possible may be obtained by inspection of figure 2, and the results are given in table 1. As the mean-flow velocity increases from zero, the first mode sounds at $U_{min} = 6{\cdot}36\,\mathrm{m\,s^{-1}}$. The prediction of U_{max} is probably relevant only as an indication of the *onset* of oscillations as the mean velocity is *decreasing* from higher values. For velocities *increasing* through U_{max} nonlinear effects are likely to control the precise point at which the mode ceases to resonate. Similarly, for velocities decreasing through U_{min}, the resonance will cease at a velocity which is somewhat *less* than U_{min}, a phenomenon which is conventionally termed hysteresis (Rockwell & Naudascher 1979). The effect of hysteresis is to extend the sounding range predicted by linear theory.

The crudest estimate of the velocity range over which a given mode will sound is obtained by neglecting *all* dissipative mechanisms and using (4.24). Such a prediction depends only on the modelling of the vortex sheet interaction with the slit, and says nothing about the values of the resonant frequencies ω_n, which may be assumed to be defined by experiment. In figure 8 we reproduce experimental results of DeMetz & Farabee (1977) giving the sounding frequency of depth modes in a wall cavity as a function of the free-stream velocity U_∞. The width $2s$ of the cavity slit was equal to 1·91 cm. Measurements indicated that, because of the mean-flow boundary layer, the phase velocity of vortical disturbances in the slit was approximately equal to $\frac{1}{2}U_\infty$. This phase velocity is precisely the mean flow velocity in the ideal, vortex sheet modelling of the slit flow described in this paper, and we shall therefore set $U = \frac{1}{2}U_\infty$ in using the inequality (4.24). Setting $f_n = \omega_n/2\pi$, (4.24) becomes

$$3{\cdot}64 f_n s < U_\infty < 7{\cdot}92 f_n s. \tag{4.26}$$

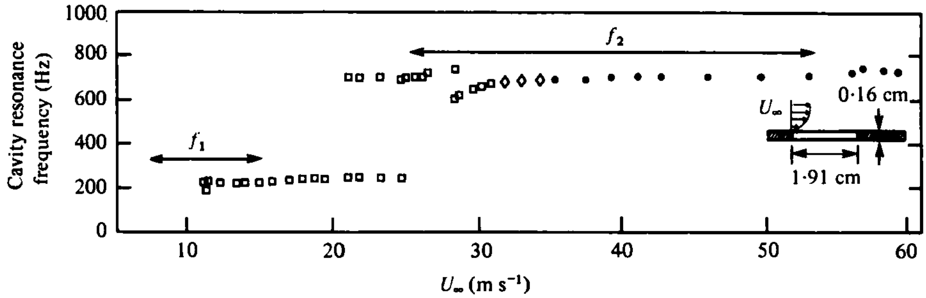

FIGURE 8. Dependence of the resonance frequency of the DeMetz & Farabee (1977) wall cavity on the mean flow velocity. The solid lines represent the velocity ranges predicted by (4.26) in which the resonance frequencies f_1 = 200 Hz and f_2 = 700 Hz are excited by the flow. □, laminar boundary layer; ◇, intermittent transition boundary layer; ●, turbulent boundary layer.

f_n (Hz)	$(U_\infty)_{min}$ (m s^{-1})	$(U_\infty)_{max}$ (m s^{-1})
200	6·95	15·13
700	24·33	52·92

TABLE 2

Investigator	$2s/\lambda$	Remarks
Rossiter (1962)	0·75	Square well cavity
DeMetz & Farabee (1977)	0·67	Turbulent boundary layer
	0·33	Laminar boundary layer
Elder (1978)	0·48–0·76	
Hersh & Walker (1979)	0·52	Circular aperture

TABLE 3

Two frequencies were involved in the experiment, namely 200 and 700 Hz, and their respective ranges of excitation predicted by (4.26) are given in table 2. These results are indicated by the solid lines in figure 8. The extent of the order-of-magnitude agreement between the predictions of the ideal, linear theory and experiment is remarkable.

It was pointed out at the end of § 2, (2.31), that $\mathrm{Im}(-F) > 0$ within the interval $0{\cdot}5 \lesssim 2s/\lambda \lesssim 1{\cdot}1$, (where λ is the hydrodynamic wavelength of the disturbance in the slit), and attains its maximum value at $2s/\lambda \simeq \frac{3}{4}$. The value of this ratio at resonance has been measured by several investigators, and their results are collected together in table 3 for comparison with the theory. The experiments of Hersh & Walker (1979) actually involved a circular aperture, and only a rough order-of-magnitude comparison is possible. To do this the radius of the aperture has been set equal to s, and the phase velocity of the vortical disturbances is taken to equal one-half of the measured free-stream velocity.

5. Conclusion

The linear theory of the interaction of a mean shear layer with a two-dimensional aperture reveals that a proper modelling of the flow requires that the Kutta condition be imposed at the leading or upstream edge. The displacement of the shear layer is then predicted to be weakly singular at the trailing edge, and it has been argued that this constitutes the linear-theory analogue of the violent motion which is known from experiment to occur there. If the Kutta condition is not applied (so that additional vortex shedding does not occur) we have shown that, on the basis of linear theory, an exchange of energy between the mean and unsteady components of the flow is not possible. This is in accord with previous theoretical findings in analogous flow/surface interaction problems (Bechert 1979; Howe 1979*a*, *b*, 1980*a*, *b*), and a simple dynamical discussion of the energy exchange mechanism has recently been given by the author (Howe 1980*c*). Similarly, the application of the Kutta condition is a crucial element in the theoretical explanation of the spontaneous excitation and suppression of wall-cavity oscillations.

Finally, it may be wondered whether the present theory also provides a theoretical model of edge-tone generation by a semi-infinite jet. This does *not* appear to be the case. Indeed, it follows easily from the results of § 4, with the cavity removed and the region in $x_2 < 0$ assumed to be filled with stagnant fluid, that

$$a_+ = a_- = \pi^{-1}\ln(se/2d) - ikd/2\pi, \tag{5.1}$$

and that the eigenfrequencies of the edge tone satisfy

$$F(\omega s/U) + \ln(4d/es) + i\omega d/2c = 0. \tag{5.2}$$

For real ω this implies that

$$\operatorname{Re} F(\omega s/U) + \ln(4d/es) = 0, \tag{5.3a}$$

$$\operatorname{Im} F(\omega s/U) + \omega d/2c = 0. \tag{5.3b}$$

The second of these requires that $\operatorname{Im}(F) < 0$, i.e. that $1{\cdot}59 < \omega s/U < 3{\cdot}49$, in which case (cf. figure 2) $1{\cdot}2 < -Re(F) < 1{\cdot}9$. This means that (5.3*a*) can be satisfied only for aspect ratios $d/2s$ such that

$$1{\cdot}13 < d/2s < 2{\cdot}27. \tag{5.4}$$

In this case $\epsilon_0 \equiv \omega s/U$ is fixed by (5.3*a*), which then yields the value of $\operatorname{Im} F(\epsilon_0)$ and, for given sound speed in (5.3*b*), the resonant frequency $\omega_0 = -(2/d)\operatorname{Im} F(\epsilon_0)$. This resonance occurs when the flow velocity U is equal to $-(2cs/d)\operatorname{Im}\{F(\epsilon_0)/\epsilon_0\}$.

The theory accordingly predicts that the edge tone sounds at a single frequency ω_0 and at a unique value of the mean-flow velocity U. There is no obvious connection between this and experimental observations of the type reported by Rockwell & Naudascher (1979) which exhibit a range of frequencies and velocities of operation of the edge tone. It is doubtful if the present theory is at all relevant, especially in view of the rigid limits placed on the aspect ratio by (5.4). A successful theory of the edge tone has been proposed by Crighton & Innes (1981), which predicts the dependence of the edge-tone frequency on the mean-flow velocity. Their analysis involved the formulation and solution of a three-part Wiener–Hopf problem together with an application of the Kutta condition at the upstream edge of the aperture, and assumed the acoustic wavelength to be much *smaller* than the aperture width $2s$.

REFERENCES

Ashley, H. & Landahl, M. 1965 *Aerodynamics of Wings and Bodies*. Addison-Wesley.

Barthel, F. 1958 Investigations on nonlinear Helmholtz resonators. *Frequenz* **12**, 1–11.

Bechert, D. 1979 Sound absorption caused by vorticity shedding, demonstrated with a jet flow. *A.I.A.A. paper* 79–0575.

Bechert, D., Michel, U. & Pfizenmaier, E. 1977 Experiments on the transmission of sound through jets. *A.I.A.A. paper* 77–1278.

Carrier, G. F., Krook, M. & Pearson, C. E. 1966 *Functions of a Complex Variable*. McGraw-Hill.

Covert, E. E. 1970 An approximate calculation of the onset velocity of cavity oscillations. *A.I.A.A. J.* **8**, 2189–2194.

Crighton, D. G. & Innes, D. 1981 Analytical models for shear layer feed-back cycles. *A.I.A.A. paper* 81–0061.

DeMetz, F. C. & Farabee, T. M. 1977 Laminar and turbulent shear flow induced resonances. *A.I.A.A. paper* 77–1293.

Elder, S. A. 1978 Self-excited depth mode resonance for a wall-mounted cavity in turbulent flow. *J. Acoust. Soc. Am.* **64**, 877–890.

Fletcher, N. H. 1979 Air flow and sound generation in musical instruments. *Ann. Rev. Fluid Mech.* **11**, 123–146.

Gradshteyn, I. S. & Ryzhik, I. M. 1965 *Table of Integrals, Series and Products*. Academic.

Heller, H. H. & Bliss, D. B. 1975 The physical mechanism of flow-induced pressure fluctuations in cavities and concepts for their suppression. *A.I.A.A. paper* 75–491.

Hersh, A. S. & Walker, B. 1979 Effect of grazing flow on the acoustic impedance of Helmholtz resonators consisting of single and clustered orifices. *N.A.S.A.* CR 3177.

Howe, M. S. 1979*a* Attenuation of sound in a low Mach number nozzle flow. *J. Fluid Mech.* **91**, 209–230.

Howe, M. S. 1979*b* On the theory of unsteady high Reynolds number flow through a circular aperture. *Proc. Roy. Soc.* A **366**, 205–223.

Howe, M. S. 1980*a* The influence of vortex shedding on the diffraction of sound by a perforated screen. *J. Fluid Mech.* **97**, 641–653.

Howe, M. S. 1980*b* On the diffraction of sound by a screen with circular apertures in the presence of a low Mach number grazing flow. *Proc. Roy. Soc.* A **374**, 543–568.

Howe, M. S. 1980*c* The dissipation of sound at an edge. *J. Sound Vib.* **70**, 407–411.

Landau, L. D. & Lifshitz, E. M. 1959 *Fluid Mechanics*. Pergamon.

Milne-Thomson, L. M. 1968 *Theoretical Hydrodynamics*, 5th edn. Macmillan.

Möhring, W. 1975 On flows with vortex sheets and solid plates. *J. Sound Vib.* **38**, 403–412.

Rockwell, D. & Naudascher, E. 1979 Self-sustained oscillations of impinging free shear layers. *Ann. Rev. Fluid Mech.* **11**, 67–94.

Ronneberger, D. 1972 The acoustical impedance of holes in the wall of flow ducts. *J. Sound Vib.* **24**, 133–150.

Rossiter, J. E. 1962 The effect of cavities on the buffeting of aircraft. *Royal Aircraft Est. Tech. Memo.* Aero 754.

Tam, C. K. W. & Block, P. J. W. 1978 On the tones and pressure oscillations induced by flow over rectangular cavities. *J. Fluid Mech.* **89**, 373–399.